Preprint Title Determination of the molecular structure and (*m*,*n*) index assignment to the constituent walls of MWCNTs with undetermined diameters and chirality

Authors Viktor Andonovic, Aleksandar T. Dimitrov, Perica Paunovic and Beti Andonovic

Publication Date 20 Nov 2020

Article Type Full Research Paper

ORCID® iDs Aleksandar T. Dimitrov - https://orcid.org/0000-0002-8845-0641; Beti Andonovic - https://orcid.org/0000-0002-5386-457X

Determination of the molecular structure and (*m*,*n*) index assignment to the constituent walls of MWCNTs with undetermined diameters and chirality

Viktor Andonovic[1], Aleksandar T. Dimitrov[2], Perica Paunovic[2], Beti Andonovic[2*]

[1] Jožef Stefan Institute, Jamova cesta 39, Ljubljana, 1000, Slovenia

[2] Faculty of Technology and Metallurgy, University "St Cyril and Methodius", Rugjer Boskovik 16, Skopje, 1000, North Macedonia

Email: Beti Andonovic[*] – beti@tmf.ukim.edu.mk

* Corresponding author

Abstract. Each carbon nanotube (CNT) has its own mathematical representation due to its hexagonal lattice structure. The subjects of research are multi-wall carbon nanotubes (MWCNTs) and determining their structural parameters: innermost and outermost diameters, chiral indices *m* and *n*, number of walls and their unit cell parameters. Within this paper low frequency region and corresponding high frequency parts of Raman spectra of three experimentally produced CNTs are considered, as well as use of Python programming for the most accurate (*m*,*n*) assignment. Determining the chirality of these samples enables calculation of other structural properties which are performed hereby. Furthermore, this author's work enables future studies on the samples, as are calculation of different topological indices using the graph representation and the chirality of the studied CNT samples.

Key words: chirality; indices; MWCNT; Python; Raman spectra

INTRODUCTION

Carbon nanotubes (CNTs) are one of the several allotropes of carbon in nanodimensions (1 nm = 10^{-9} m) with highly outstanding properties. Since graphene is a 2D building unit of all carbon allotropes such as fullerenes, CNTs, nanoribbons, and so on, CNTs may be geometrically observed as wrapped

up graphene structure having seamless cylindrical shape. Each nanotube has its own mathematical representation due to its hexagonal lattice structure [1],[2]. The geometric structure analysis of carbon nanotubes has been quite a challenging task, particularly if the subject of research is multi-wall carbon nanotubes (MWCNTs) [1]-[3], [5]-[8]. Knowing CNTs structural parameters (diameter, chiral angle, chiral indices *m* and *n*) is basically knowing their properties, which is essential for any research in the field of CNTs and their application. There are several excellent tools as are HRTEM, ED, RRS and others that suggest some models of (*m*,*n*) assignment for single-wall carbon nanotubes (SWCNTs), as well as for MWCNTs [5]. However, precise determination of the CNTs molecular structure features becomes extremely complicated for multi-walled tubes, even when there are just few walls (layers) [6], [7]. Thorough and overall analysis and use of experimental results combined with recent theoretical background may lead to successful estimation of its structural elements.

There are different experimental methods of producing CNTs, and based on several factors, the obtained tubes may be either SWCNTs or MWCNTs. The CNT with the lowest reported diameter value experimentally produced is known to have the diameter $d_k = 4\text{Å}$ [10]. It is the narrowest attainable nanotube that can still remain energetically stable. Such nanotubes may be the innermost constituent layer of MWCNTs. In contrast to CNTs with larger diameters, whose conductivity nature depends on their diameter and chirality, these smallest nanotubes are always metallic, regardless of the chirality [10]. Within this paper Raman spectra of three experimentally produced commercial CNTs of undetermined diameter, chirality, and number of walls, are considered. They are assigned the following nomenclatures: CNT_1, CNT_2, and CNT_3. Due to the fact that their properties are tightly connected and dependent on their atomic structure, detailed analyses with regard to determining their diameters is performed, as well as calculating their chiral indices *m* and *n*, and furthermore other parameters, hence estimating the number of walls of each nanotube. This research was strictly focused to determination of outermost and innermost diameters, as much as to assigning the corresponding chiral indices to the tubes' walls, estimation of the number of other inner diameters, which would further implicate the number and the conductive nature of the walls. Authors strongly suggest future studies on the samples, as are performing additional EDP analysis to enhance and confirm the accuracy of applied methods, as

well as estimation of distance based topological indices (Wiener, Harary, Balaban, Sum-Balaban, Gutman, etc.), since it is known that they are related to some properties of the corresponding molecules. The latter is possible by using the graph representation and the chirality of the studied samples [8].

RESULTS AND DISCUSSIONS

The analysis and the approaches to the considered nanotubes, are thoroughly described and discussed with regard to CNT_1, CNT_2, and CNT_3.

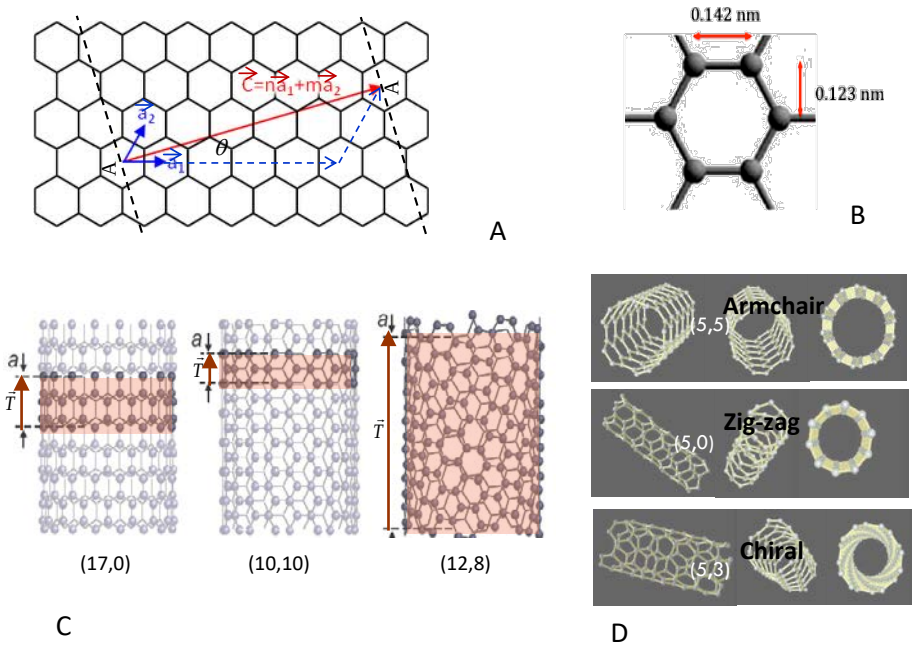

Figure 1: A) Atomic mathematical CNT structure; B) CNT constants; C) Various CNT unit cells; D) Examples of the three CNT types according to θ.

For a mathematical representation of CNTs and due to its hexagonal lattice atomic structure, one can use the relations among various CNT parameters reported in numerous works, as are [1]: unit vectors $\vec{a}_1$ and $\vec{a}_2$, chiral vector $\vec{C}_h$, CNT diameter d_{CNT}, chiral angle θ, translation vector $\vec{T}$ of the CNT unit cell (being the shortest repeat distance along the nanotube axis), number of hexagons N_H, number of vertices (atoms) N_V and so on, (Fig. 1), which are expressed with the formulas (1)-(5) in the experimental part. Lattice constants are the lengths of the unit vectors $a = |\vec{a}_1| = |\vec{a}_2| = 0.246$ nm, and the distances between neighbouring carbon atoms are $a_{C-C} = 0.142$ nm.

For each CNT other than the narrowest reported one of $d_k = 4\text{Å}$, it holds that it is metallic, if and only if it satisfies the condition $\text{MOD}(2m+n,3)=0$. To date, the determination of molecular geometric structure of carbon nanotubes and its analysis has been quite a challenging task, even for SWCNTs that are undetermined and particularly for MWCNTs. Each of the three nanotubes CNT_1, CNT_2, and CNT_3 is undetermined with regard to its diameter, chirality and number of walls. In Fig. 2 there are shown TEM and SEM images of the tubes, and it is evident that these nanotubes are of highly different diameters, which are undetermined, as is also their chirality.

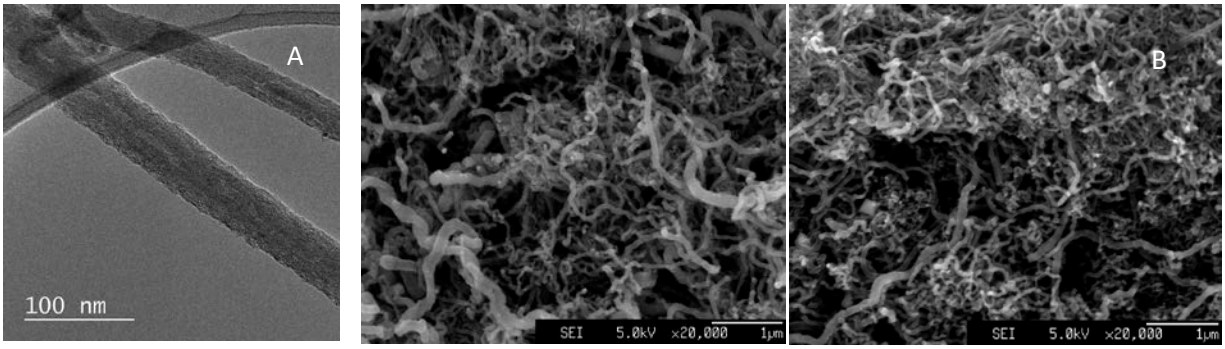

Figure 2: A) TEM image of MWCNTs; B) SEM images of MWCNTs of undetermined diameters and chirality

This research is focused to determination of their diameters, both innermost and outermost diameters denoted by d_i and d_o correspondingly, determination of chiral indices (*m*,*n*), the total number and conductive nature of other inner walls having a diameter d_k, and the interlayer distance δ_r^k (Fig. 3). The latter are known to usually be within the interval $0.32\,\text{nm} \le \delta_r^k \le 0.35\,\text{nm}$, although it can sometimes vary from $0.27\,\text{nm}$ up to $0.35\,\text{nm}$ [9].

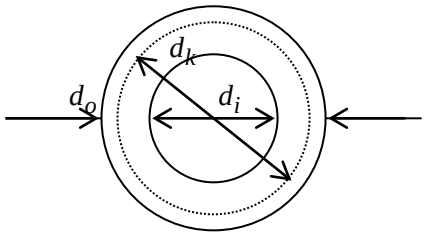

Figure 3: Diameters of MWCNTs

The relation among the diameters and the interlayer distances is given by $\delta_r^k = \frac{d_k - d_{k-1}}{2}$, whereas $N = \frac{d_o - d_i}{2\delta_r} + 1$ describes the relation among the number of layers *N*, the innermost diameter d_i, the outermost diameter d_o, and the average interlayer distance δ_r.

The key role in the analysis was assigned to the Raman spectra within two frequency regions of each nanotube sample: $\omega \in [50\ \mathrm{cm}^{-1}, 350\ \mathrm{cm}^{-1}]$ and $\omega \in [1200\ \mathrm{cm}^{-1}, 1800\ \mathrm{cm}^{-1}]$. The first region was expected to point to the Radial breathing mode (RBM) frequencies for SWCNTs, or to Radial breathing-like mode frequencies (RBLM) for MWCNTs. These measurements can be used as an excellent tool to estimate the diameters of each layer of the tubes, since RBM is an active mode where all carbon atoms move in-phase in the radial direction. To date, several experimental relations have been established between the diameter of the tube and the RBM frequency ω_{RBM} [5]. This work uses two equations (6) and (7), depending on the studied samples Raman data, since those relations are equivalent only within a limited range of diameters. While (6) shows the dependence of the innermost diameter d_i and the outermost diameter d_o on the corresponding frequencies, and is more accurate when small diameters are considered, (7) can be used for much larger range of diameters and is more useful when it comes to very large diameters (or extremely low frequencies). Hence it will be used whenever relation (6) is unusable or unreliable due to the size of the outermost diameter. One may notice that d_i is obtained by the same equation as d_o, with C_e being 0. The latter is due to the fact that the parameter C_e is used whenever there are environmental conditions around the nanotube [1],[5]. The innermost concentric nanotube within the MWCNT is not affected by such conditions, which is not the case with the outermost concentric tube. Obtaining possible (*m*,*n*) candidates to satisfy equation (2) and the number of these pairs was performed by using Python programming. The Python code is given in Table 1. The final choice of (*m*,*n*) assignment is made by the analysis of the G-peak.

Table 1: Python code for determining (*m*,*n*)

```
def mn_pairs(diameter, interval):
```

```
    count=0
    m_n=[]
    for m in range(1,int((diameter/0.079)+1)):
      for n in range(0,m+1):
        if((0.079*math.sqrt(n*n+m*m+n*m))>=((diameter-interval))
and (0.079*math.sqrt(n*n+m*m+n*m))<=((diameter+interval))):
            count+=1
            m_n.append((m,n))
    print(count, "(m,n)")
    return m_n
```

The high frequency region of G-modes, showing off in the interval $\omega \in (1500\ \mathrm{cm}^{-1}, 1600\ \mathrm{cm}^{-1})$, is used to help the overall analysis. In Fig. 4, D and G-modes of the studied samples are presented. Although it is not relevant for this research, one may notice that the ratio of their intensities I_D/I_G for all of the three samples is relatively high, which points to CNTs' defective structure. Regarding the G-mode only, a useful diameter dependence for the chiral CNTs (semiconducting or metallic), which was here used as a control method, is given by the equations (8) and (9) [5], [11], [12].

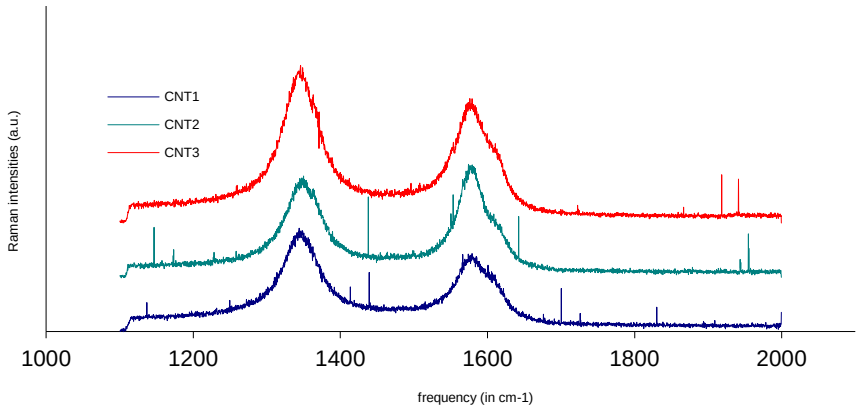

Figure 4: Raman spectra D and G-mode for CNT_1, CNT_2, and CNT_3

The number and shape of components in the G-peak are an excellent indicator of the conductive nature of the studied CNT sample. Table 2 will help the analysis when the chiral indices assignment to the samples is done [5].

Table 2: Dependence between G-peak components and the CNT conductivity

Nanotube conductivity	Components number	G-peak profile

Semiconducting chiral (SC)	2	LO: narrow, symmetric
		TO: narrow, symmetric
Metallic chiral (MC)	2	LO: broad, asymmetric
		TO: narrow, symmetric
Armchair	1	TO: narrow, symmetric
Semiconducting zigzag (SZ)	1	LO: narrow, symmetric
Metallic zigzag (MZ)	1	LO: broad, symmetric

NANOTUBE CNT_1. (n,m) ASSIGNMENT RESULTS

The Raman spectra in both frequency regions for CNT_1 are shown in Fig. 5 A, B. There is only one peak in the low frequency region, which indicates that the nanotube is a single-wall, i.e. $d^{(1)} = d_o^{(1)}$. Using (6), it is obtained $d^{(1)} = d_o^{(1)} = 0.665\,\text{nm}$.

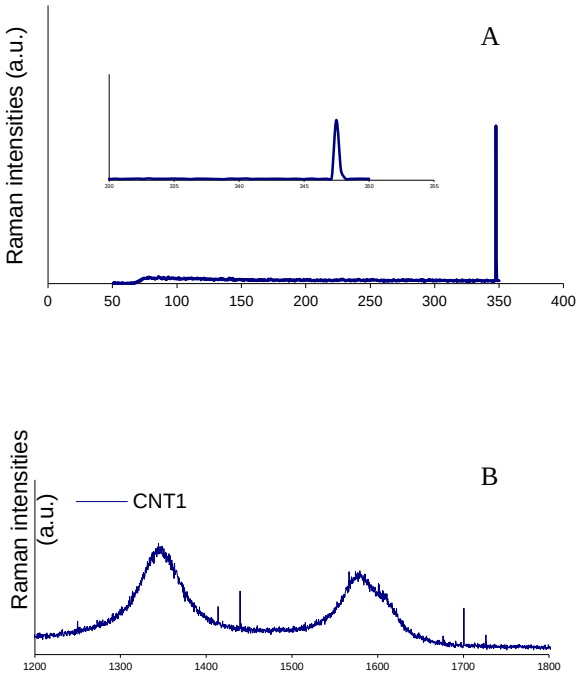

Figure 5: A) Raman spectrum RBM for CNT_1;
B) Raman spectrum G-mode for CNT_1

The determined diameter is lower than 1 nm and the most accurate results are expected for diameters 1 nm – 2.5 nm, hence the determining possible chiral indices candidates was performed within somewhat broader diameter interval $(d^{(1)} - 0.02, d^{(1)} + 0.02)$. Python programming was applied for obtaining possible candidates, and the resulting 24 possibilities are indicated in Table 3.

Table 3: Possible (*m*,*n*) assignments for diameter $d^{(1)} = 0.665$ nm of CNT_1

(4,3)	(4,4)	(5,2)	(5,3)	(5,4)	(5,5)
(6,0)	(6,1)	(6,2)	(6,3)	(6,4)	(6,5)
(6,6)	(7,0)	(7,1)	(7,2)	(7,3)	(7,4)
(7,5)	(8,0)	(8,1)	(8,2)	(8,3)	(8,4)

Due to the broadness of the G-peak (see Fig. 5 B), the chiral indices candidate pairs need to satisfy the metallic condition $\mathrm{MOD}(2m+n,3)=0$. Hence, only the five chiral indices pairs in red (see Table 3) are considered. However, the armchair type (5,5) would show one narrow and symmetric G-peak, and the chiral metallic (6,3), (7,1), and (8,2) would show two components of the G-peak, one being narrow (see Table 2), which here is not the case.

This leaves only one possibility, the zig-zag metallic tube (6,0), which is in high accordance with the broad and asymmetric G-peak of the nanotube CNT_1.

In Figure 6 there is an illustration of CNT_1 with determined diameter and chiral indices assignment.

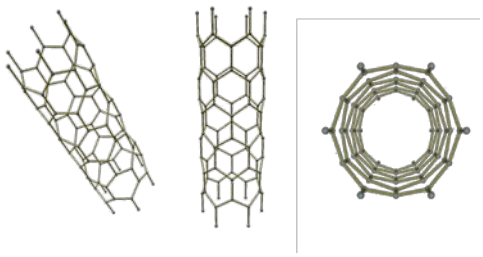

Figure 6: Visual model of (6,0) SWCNT

NANOTUBE CNT_2. (n,m) ASSIGNMENT RESULTS

The Raman spectra in RBLM frequency region, as well as in G-mode region for CNT_2 are shown in Fig. 7 A, B. There are two peaks in the low frequency range, which identifies the CNT_2 as double-wall CNT (DWCNT).

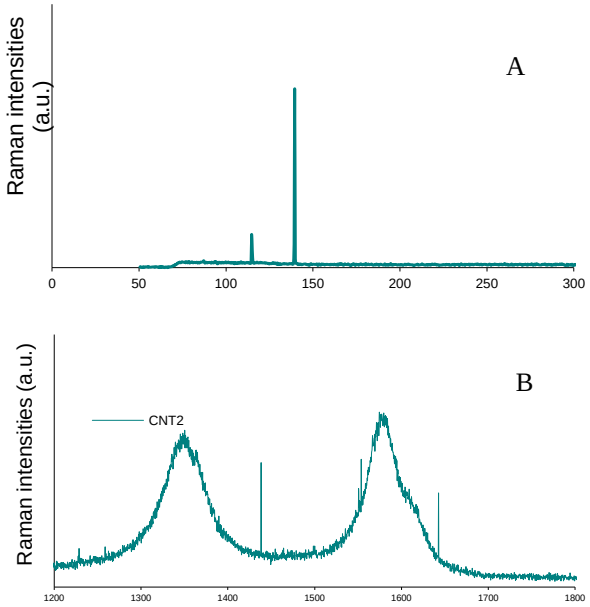

Figure 7: A) Raman spectrum RBLM for CNT_2;
B) Raman spectrum G-mode for CNT_2

According to the corresponding frequency values in Fig.7 A and equation (6), both the innermost and outermost diameters are calculated as $d_i^{(2)} = 1.63\,\text{nm}$ and $d_o^{(2)} = 2.3\,\text{nm}$.

The interlayer distance is calculated as $\delta_r = \frac{d_o - d_i}{2} = 0.335\,\text{nm}$, which accurately fits the equilibrium distance for tubes that are DWCNTs [5].

With regard to the G-peak and the chirality of each constituent SWNT, one expects to observe 4 (Ch@Ch), 3 (Ch@ACh or ACh@Ch) or 2 (ACh@ACh) components in the Raman spectrum data of any DWNT [5]. However, some components can appear at very close frequencies, and therefore cannot be easily differentiated. Hence, the number of observed components can be less than the number expected for certain sample structure (see Table 2). Considering CNT_2, two identified components of the G-peak are located at the frequencies 1570.98 cm^{-1} and 1574 cm^{-1}. These frequencies enable the estimating of the diameters, and consequently the following was obtained: $d_i^{(2)} = 1.58\,\text{nm}$ by using equation (8), which implicates a semiconducting chiral (SC) layer, and $d_o^{(2)} = 2.25\,\text{nm}$ by using equation (9), which implicates a metallic chiral (MC) layer. One may notice that the obtained diameters by both methods are in high accordance, and the values obtained by (6) are kept as accurate.

The determined diameters are within 1 nm – 2.5 nm, hence the interval for calculating possible chiral indices candidates was performed within narrower diameter interval with a 0.01 nm error bar $(d^{(2)} - 0.01, d^{(2)} + 0.01)$. Python programming was applied for obtaining possible assignment candidates for both diameters to satisfy equation (2), and the results of 16 combinations are derived from the pairs indicated in Table 4.

Table 4: Possible (*m*,*n*) assignments for the innermost and outermost diameters of CNT_2

$d_o^{(2)}$	$d_i^{(2)}$
(22,11)	(12,12)
(25,7)	(13,11)
(27,4)	(17,6)
(28,2)	(19,3)

Qualitative analysis of the G-peak indicated a broad component, hence a metallic chiral character of one layer and semiconducting chiral character of the other layer. Hence, the possible cases are either MC@SC or SC@MC, which corresponds to the implications from equations (8) and (9) results. The only chiral indices pair satisfying the MC condition is (25,7). There are three possibilities of type SC@MC: (13,11)@(25,7), (17,6)@(25,7), and (19,3)@(25,7). The exact innermost and outermost diameters of these three possibilities give interlayer distances 0.329 nm, 0.335 nm, and 0,335 nm correspondingly. The latter eliminates the first tube, and the remaining two possibilities (17,6)@(25,7), and (19,3)@(25,7) are equally possible up to this point. However, it is possible to make a strong distinction between these two possibilities by an additional method of performing and analyzing an EDP of the CNT_2. Authors suggest such further research, since this analysis would estimate the ratio *m*/*n* [5], which greatly differs at the last two possibilities. It is highly expected that it would leave only one candidate combination.

In Fig. 8 there is an illustration of the two candidates with determined diameters and chiral indices assignment to the tube CNT_2.

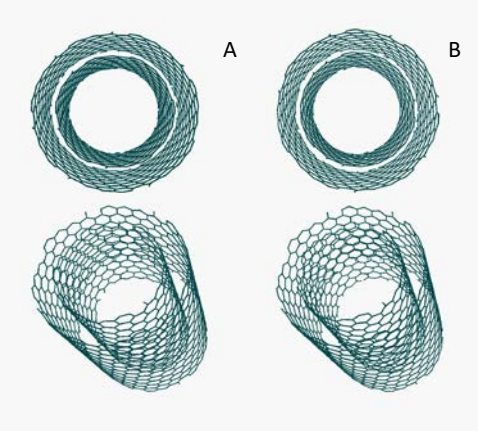

Figure 8: Visual model of DWCNT
A) (17,6)@(25,7); B) (19,3)@(25,7)

NANOTUBE CNT_3. (n,m) ASSIGNMENT RESULTS

Several (six) peaks may be noticed in the Raman spectrum in RBLM frequency region of CNT_3 (Fig. 9 A), which identifies this nanotube as MWCNT. Presence of both narrow and broad components in the G-mode range (Fig. 9 B) implicates both semiconducting and metallic layer in the structure of CNT_3. According to the corresponding frequency values in Fig. 9 A and equation (6), both the innermost and outermost diameters are calculated as $d_i^{(3)} = 0.65$ nm and $d_o^{(3)} = 7.73$ nm .

The frequency of the outermost diameter $d_o^{(3)}$ is extremely low and near the limit of possible calculation, therefore its calculation may have a high error bar or even be highly inaccurate. Hence, the outermost diameter is recalculated using equation (7) it is obtained that $d_o^{(3)} = 4.04$ nm

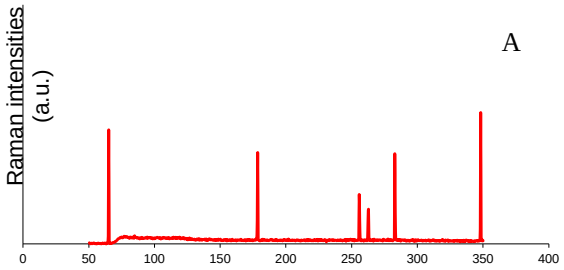

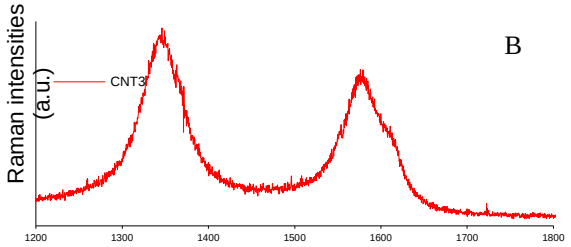

Figure 9: A) Raman spectrum RBLM for CNT_3;
B) Raman spectrum G-mode for CNT_3

To be able to decide which outermost diameter value is good, equation (8) is applied for the G-peak component frequency $\omega = 1580.34\,\mathrm{cm}^{-1}$. Thus it is obtained $d_o^{(3)} = 4.07\,\mathrm{nm}$. The latter is in accordance with the calculated value by (7). Furthermore, the use of this equation points to semiconducting chiral layer. It is possible to estimate whether the choice of these equations was justified by checking the accordance with $N = \dfrac{d_o - d_i}{2\delta_r} + 1$, when calculating the average interlayer distance δ_r in CNT_3. Using the values N=6, $d_o^{(3)} = 4.04\,\mathrm{nm}$, and $d_i^{(3)} = 0.65\,\mathrm{nm}$, thus obtaining $\delta_r = 0.339\,\mathrm{nm}$, is an excellent indicator that the diameters are well estimated. The innermost and the outermost diameters are out of the high accuracy diameter range 1-2.5 nm, and obtained by different equations. The possible (m,n) assignment was performed using Python programming, equation (2) and corresponding error bars. For the outermost diameter, there were three possibilities in the interval $(d_o^{(3)} - 0.002,\, d_o^{(3)} + 0.002)$: (31,28), (32,27), and (49,4), each being chiral. However, considering the semiconducting nature of this layer, the only pair of chiral indices satisfying the condition $\mathrm{MOD}(2m + n, 3) \neq 0$ is (32,27).

With regard to the innermost diameter, the possible (m,n) assignment was performed in the interval $(d_i^{(3)} - 0.02,\, d_i^{(3)} + 0.02)$ resulting into two possibilities: (7,2) and (8,0), for which it must be emphasized that the pair (7,2) is within a much lower error bar. Both of these possibilities point to a semiconducting layer.

There are two possible combinations: (7,2)@@(32,27) and (8,0)@@(32,27). The option (7,2)@@(32,27) was discussed to be within a smaller error bar, and also its calculated interlayer

distance of 0.340 nm is closer to the determined $\delta_r = 0.339$ nm, than the distance of 0.341 nm that holds for the option (8,0)@@(32,27). However, these findings are not enough of a discrepancy at the latter option in order for it to be excluded.

In Fig. 10 there is an illustration of the two candidates with determined diameters and chiral indices assignment to the tube CNT_3.

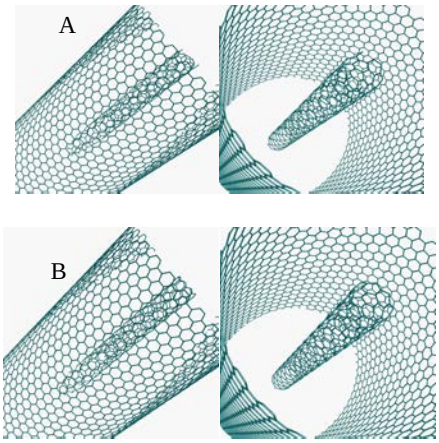

Figure 10: Visual model of
A) (7,2)@@(32,27); B) (8,0)@@(32,27)

Considering this nanotube CNT_3 it is again strongly suggested an additional EDP analysis to be performed. This would differentiate the two candidates, since they have different *m*/*n* ratios of the innermost constituent tubes, and hence it is highly expected that the EDP would leave only one possible candidate.

EXPERIMENTAL

The general equations used for determining the CNTs structures are given as follows.

$$\left|\vec{C}_h\right| = \sqrt{3}a_{C-C}(m^2 + mn + n^2)^{1/2} \text{ nm} \quad (1)$$

$$d_{CNT} = \frac{\sqrt{3}a_{C-C}(m^2 + mn + n^2)^{1/2}}{\pi}$$
$$= 0.079\sqrt{(m^2 + mn + n^2)} \text{ nm} \qquad (2)$$

$$\theta = arctg\frac{\sqrt{3}n}{2m+n},$$

$$0 \le \theta \le \frac{\pi}{6} \quad (0 \le n \le m) \quad (3)$$

$\theta = \frac{\pi}{6}$ – armchair CNT,

$\theta = 0$ – zig-zag CNT,

$0 < \theta < \frac{\pi}{6}$ – chiral CNT

$$T = \left|\vec{T}\right| = \frac{\sqrt{3}\left|\vec{C}_h\right|}{d_R} = \frac{\sqrt{3}\pi d_{CNT}}{d_R} \text{ nm}, \quad (4)$$

$d_R = GCD(2m+n, 2n+m)$, given by

$$d_R = \begin{cases} d, & \text{if } m-n \text{ is not a multiple of } 3d \\ 3d, & \text{if } m-n \text{ is a multiple of } 3d \end{cases}$$

where $d = \text{GCD}(m,n)$

$$N_{\text{H}} = \frac{2(m^2+mn+n^2)}{d_R} \quad (5)$$

$$N_{\text{V}} = \frac{4(m^2+mn+n^2)}{d_R}$$

$$d_i = \frac{228}{\omega_i^{RBLM}} \quad (6)$$

$$d_o = \frac{228}{\sqrt{(\omega_o^{RBLM})^2 - 228^2 \cdot C_e}},$$

$C_e = 0.065 \text{ nm}^{-2}$

$$\omega_{RBM} = \frac{A}{d} + B \quad (7)$$

$A = 223 \text{ cm}^{-1}$, $B = 10 \text{ cm}^{-1}$

$$\omega_{TO}^{G}(d) = 1582 - \frac{27.5}{d^2}, \quad \text{for SC} \quad (8)$$

$$\omega_{LO}^{G}(d) = 1582 - \frac{38.8}{d^2}, \quad \text{for MC} \quad (9)$$

The morphological structures of the nanotubes were investigated by TEM analysis using a FEI Tecnai G2 Spirit TWIN with a LaB6 cathode. The nanotubes were observed by scanning electron microscopy, using JEOL 6340F (SEM, 10 kV). Structural characteristics of the carbon nanostructures were studied

by means of Raman spectroscopy. Non-polarized Raman spectra were recorded by a confocal Raman spectrometer (Lab Ram ARAMIS, Horiba Jobin Yvon) operating with a laser excitation source emitting at 532 nm. The low frequency regions 50-350 cm^{-1} were taken into consideration, as well as the frequency regions 1200-1800 cm^{-1} from the Raman spectra of the CNTs. Python programming was applied to determine possible chiral indices assignment to the studied samples.

CONCLUSIONS

Based on the analysis and discussions in previous sections, it is achieved a determining of MWCNT samples by means of Raman spectroscopy data and Python programming. Although in some cases limitations occure, and particularly if the subject of research is nanotubes with more than two layers, the achievement of solely using one main tool (Raman spectroscopy) is indeed outstanding. Several important findings may be concluded:

- Determination of three CNTs' molecular structure has been performed, as well as determination of the conductive nature of the CNTs' walls; fully for CNT_1 and CNT_2, and partially for CNT_3 (as presented in Table 5);
- The thorough analyses were made using a unique approach combining the CNTs' Raman spectra in RBLM and G-mode frequency regions as a tool with employment of Python programming. The results, although with some limitations, enable working on determining ctructural characteristics of carbon nanotubes when there is just Raman spectroscopy data available;
- The performed calculations were in excellent agreement with the theoretical background and with the control methods;
- The calculations can be further improved in terms of higher certainty and results exactness, therefore corresponding methods, as is EDP, are strongly suggested;
- The results enable many applications, as well as providing full necessary information for graph theorists who work on distance-based topological indices, such as Wiener, Harary, Balaban, Sum-Balaban, Gutman, etc.

Table 5: Summarized results to specify studied CNTs

Parameters in nanotube	**CNT_1**	**CNT_2**	**CNT_3**
Chiral indices (*m*,*n*)	(6,0)	(17,6)@(25,7) (19,3)@(25,7)	(7,2)@@(32,27) (8,0)@@(32,27)
Diameters (in nm)	0.665	1.63@2.3	0.65@@4.04
Interlayer distances (in nm)	-	0.335	0.34
Number of walls	1	2	6
Conducting nature	MZ	SC@MC	SC@@SC (intrinsically Metallic)
Chiral angles (in rad)	0	0.25@0.21 0.13@0.21	0.21@@0.47 0@@0.47
Length of the unit cell (in nm)	0.6	8.87@4.17 8.87@4.17	3.54@@21.98 0.44@@21.98
Number of hexagons in the cell	12	854@566 854@566	134@@5234 16@@5234
Number of vertices in the cell	24	1708@1132 1708@1132	268@@10648 32@@10648

ACKNOWLEDGMENTS

This study was done within the following EU projects: COST Action CA17139 “European Topology Interdisciplinary Action”, and COST Action CA17140 “Cancer nanomedicine - from the bench to the bedside”.

REFERENCES

[1] M.S. Dresselhaus, G. Dresselhaus, R. Saito, A. Jorio, *Raman spectroscopy of carbon nanotubes*, Physics Reports 409 (2005), 47–99.

[2] X. Zhao, Y. Ando, L.-C. Qin, H. Kataura, Y. Maniwa, R. Saito, *Radial breathing modes of multiwalled carbon nanotubes*, Chem. Phys. Lett. 361 (2002), 169–174.

[3] C. Schwandt, A.T. Dimitrov, D.J. Fray, *High-yield synthesis of multi-walled carbon nanotubes from graphite by molten salt electrolysis*, Carbon 50 (2012), 1311–1315.

[4] B. Andonovic, A. Ademi, A. Grozdanov, P. Paunović, Aleksandar T. Dimitrov, *Enhanced model for determining the number of graphene layers and their distribution from X-ray diffraction data*, Beilstein J. Nanotechnol 6 (2015), 2113-2122.

[5] D.I. Levshov, H.N. Tran, M. Paillet, R. Arenal, X.T. Than, A.A. Zahab, Y.I. Yuzyuk, J.-L. Sauvajol, T. Michel, *Accurate determination of the chiral indices of individual carbon nanotubes by combining electron diffraction and Resonant Raman spectroscopy*, Carbon 114 (2017), 141-159.

[6] T. Natsuki, G.J.H. Melvin & Q.-Q. Ni. *Vibrational Frequencies and Raman Radial Breathing Modes of Multi-Walled Carbon Nanotubes Based on Continuum Mechanics*, Journal of Materials Science Research 2, (4) (2013).

[7] J.M. Benoit, J.P. Buisson, O. Chauvet, C. Godon, and S. Lefrant. *Low-frequency Raman studies of multiwalled carbon nanotubes: Experiments and theory*, Phys. Rev. B, 66 (7) (2002), 073417.

[8] B. Andonovic, V. Andova, T. Atanasova Pacemska, P. Paunovic, V. Andonovic, J. Djordjevic, & A. Dimitrov, *Distance based topological indices on multiwall carbon nanotubes samples obtained by electrolysis in molten salts*. BJAMI, 3(1), (2020), 7-12.

[9] O.V. Kharissova, B.I. Kharisov, *Variations of interlayer spacing in carbon nanotubes*, RSC Adv., 4, (2014), 30807-30815

[10] L. Qin, X. Zhao, K. Hirahara, et al, *The smallest carbon nanotube*, Nature 408, 50, (2000), 50-51.

[11] H. Telg, J.G. Duque, M. Staiger, X. Tu, F. Hennrich, M.M. Kappes, et al., *Chiral index dependence of the G+ and G- Raman modes in semiconducting carbon nanotubes*, ACS Nano 6 (2012), 904-911.

[12] V. Popov, P. Lambin, *Radius and chirality dependence of the radial breathing mode and the G-band phonon modes of single-walled carbon nanotubes*, Phys. Rev. B 73, (2006), 085407.